DETERMINATION OF AN AEROSOL DISPERSE COMPOSITION FROM MEASUREMENTS OF THE OPTICAL TRANSFER FUNCTION OF A MEDIUM WITH ALLOWANCE FOR MULTIPLE SCATTERING IN THE SMALL–ANGLE APPROXIMATION

V.V. Veretennikov

Institute of Atmospheric Optics,
Siberian Branch of the Russian Academy of Sciences, Tomsk
Received May 31, 1993

A new technique for reconstructing the particle size distribution from the data on the optical transfer function in the small–angle approximation of the radiation transfer theory is considered. The technique uses a representation of the Fourier transform of the aerosol scattering phase function in the form of a correlation function of particle shadow. The accuracy of the method is analyzed numerically based on the developed regularizing algorithm for the inverse problem solution. It is shown that the accuracy of the method is the same as of the solution for the inverse problem on angular distribution of multiply scattered plane wave.

The integral equation derived in Ref. 1 enables one to determine the spatial distribution of the extinction coefficient for a given microstructure of a medium or, on the other hand, to reconstruct the particle size distribution function for a given profile of the extinction coefficient retrieved from the data on the optical transfer function (OTF) of the medium in the small–angle approximation of the radiative transfer equation (RTE). The first problem was considered at length in Ref. 1. This paper deals with the analysis of the second problem, the solution of which is based on the fruitful idea of representation of the Fourier transform of the scattering phase function as a correlation function of particle shadow proposed in Ref. 2. This idea was previously used to advantage in developing the method for diagnostics of coarsely dispersed media from measurements of the angular distribution of multiply scattered radiation in the small–angle approximation.[3]

1. INITIAL EQUATIONS AND PROBLEM FORMULATION

In solving the RTE in the small–angle approximation,[2,4,5] the Fourier transform of the scattering phase function can be represented in the form of an autocorrelation function of mean particle shadow[2,3]

$$\varphi(\rho) = \int\limits_{\rho/2}^{R} G\,(\rho/2r)\, f(r)\, \mathrm{d}r\ , \qquad (1)$$

where $f(r) = s(r)/S$, $s(r) = \pi r^2 n(r)$, and $n(r)$ is the distribution of particle number density over size; $S = \int\limits_0^R s(r)\,\mathrm{d}r$ is the total geometric cross section of particles in unit volume of the scattering medium; and, $G(\rho/2\,r)$ is the autocorrelation coefficient of the ratio of shadow of a spherical particle of radius r to its cross sectional area

$$G(t) = \begin{cases} 2\pi^{-1}\,[\arccos t - t\sqrt{1-t^2}\,]\ , & t \le 1, \\ 0, & t > 1. \end{cases} \qquad (2)$$

The dependence $\varphi(\rho)$ can be found from the angular distribution of a multiply scattered plane wave[3] or from measurements of a spatial intensity correlation function.[6] In its turn, with knowledge of the function $\varphi(\rho)$, it is possible to formulate an inverse problem in reconstructing the microstructure of the medium from integral equation (1). Such a problem was considered in Ref. 6 where the method of numerical inversion of Eq. (1) was proposed and its efficiency was analyzed.

In this paper a new method is proposed for determining a disperse composition of a dense medium from the measurements of its OTF E(ν) which in small–angle approximation of the RTE is related to the autocorrelation function of a particle shadow $\varphi(\rho)$ via the expression[1]

$$F(\nu) = \exp\{-\mathrm{t} + g(\mathrm{n})/2\}\ , \qquad (3)$$

where

$$g(\nu) = \int\limits_0^z \varepsilon(z-t)\, \varphi\,(\nu t/\kappa)\, \mathrm{d}t\ , \qquad (4)$$

ν is the spatial frequency, τ is the optical depth of the medium in the interval $[0, z]$, and $\varepsilon(t)$ is the volume extinction coefficient.

In the general case the function $g(\nu)$ given by Eq. (4) depends on spatial distribution of the extinction coefficient. However, for a homogeneous medium with the constant extinction coefficient $\varepsilon(t) = \varepsilon$ along the path, expression (4) is simplified

$$g(\nu) = \varepsilon \int\limits_0^z \varphi\,(\nu t/\kappa)\, \mathrm{d}t\ . \qquad (5)$$

By substituting the variables $\rho' = \nu t/\kappa$ and $\rho = \nu z/\kappa$ in Eq. (5) we obtain the integral equation

$$\int\limits_0^{\mathrm{r}} \varphi\,(\rho')\, d\rho' = h(\rho)\ , \qquad (6)$$

where $h(\rho) = \tau^{-1}\rho g(\kappa\rho/z)$, from which the correlation function of particle shadow $\varphi(\rho) = dh(\rho)/d\rho$ is found. Thus the problem in reconstructing the particle size distribution function $f(r)$ from measurements of the OTF of a medium $F(\nu)$, given by Eq. (3), with the known optical depth τ necessitates the differentiation of the function $g(\nu) = 2\,[\tau + \ln F(\nu)]$ with subsequent inversion of integral equation (1). The optical depth τ is uniquely determined by the value of the net radiation flux propagating through a plane perpendicular to the direction of propagation $\tau = -\ln F^2(0)$, where

$$F(0) = 2\pi \int_0^\infty E(r)\, r\, dr\,, \tag{7}$$

$E(r)$ is the radial distribution of the irradiance in the plane $z = \text{const}$.

2. DETERMINATION OF MOMENTS OF DISTRIBUTION AND THE INVERSION PROCEDURE

2.1. Some important characteristics of the unknown distribution $f(r)$ can be found without inversion of Eq. (1). It follows from the properties of the function $\varphi(\rho)$ determined by its kernel $G(t)$ in the form of Eq. (2) that $h(\rho)$ is a positive function, increasing smoothly and being convex upwards when $0 < \rho \le 2R$, which has a maximum of

$$h_{\max} = \int_0^{2R} \varphi(\rho)\, d\rho = \frac{8}{3\pi}\,\overline{r} \tag{8}$$

for $\rho > 2R$, where $\overline{r} = \int_0^R r\, f(r)\, dr$ is the particle radius averaged over the distribution $f(r)$. Thus the maximum of the function $h(\rho)$ determines the mean particle radius. Analogous result was obtained in Ref. 7 where a simplified representation of integral (4), being valid for small ν, was used.

Let us integrate the function $h(\rho)$ from 0 to $2R$

$$H = \int_0^{2R} h(\rho)\, d\rho = 2R \int_0^{2R} \varphi(\rho)\, d\rho - \int_0^{2R} \rho\, \varphi(\rho)\, d\rho\,. \tag{9}$$

The first integral in the right side of Eq. (9) is found from formula (8). The second integral is calculated by substituting the expression for $\varphi(\rho)$ in the form of Eq. (1) in it and changing the order of integration. The result is

$$\int_0^{2R} \rho\, \varphi(\rho)\, d\rho = \frac{1}{2} \int_0^{R} f(r)\, r^2\, dr = \overline{r^2}/2\,. \tag{10}$$

From Eqs. (8)–(10) the expression for determining the rms particle radius is finally derived

$$\overline{r^2} = 2\,(2Rh_{\max} - H) \tag{11}$$

based on the data on the function $h(\rho)$. In analogous way we may obtain the relations for higher–order moments of the distribution $f(r)$.

2.2. To eliminate the necessity for the solution of two ill–posed problems in reconstructing the function $f(r)$ [differentiation of $h(\rho)$ and inversion of integral equation (1)], an alternative approach is proposed in this paper. Let us first transform to the dimensionless variable $\eta = r/R$, $0 \le \eta \le 1$ in Eq. (1). Substituting then Eq. (1) into Eq. (5) and changing the order of integration, we obtain the integral equation

$$\int_0^1 Q(\xi/\eta)\, \tilde{f}(\eta)\, \eta\, d\eta = \tilde{h}(\xi), \qquad 0 \le \xi \le 1\,, \tag{12}$$

where the unknown function $\tilde{f}(\eta) = R\, f(R\eta)$ has a meaning of normalized distribution of particles over relative size of geometric cross section η, $\xi = p\nu$, $p = z/2\kappa R$, right side $\tilde{h}(\xi) = h(2R\xi)/2R$, and the kernel

$$Q(x) = \begin{cases} c + \dfrac{2}{\pi}\,[x \cdot \arccos(x) - y - y^3/3]\,, & x \le 1, \\ c\,, & x > 1 \end{cases} \tag{13}$$

$c = 4\pi/3$, $y = (1 - x^2)^{1/2}$.

Now we consider the properties of the kernel $Q(\xi/\eta)$ in the form of Eq. (13) in the domain $\Omega = \{0 \le \xi \le 1,\ 0 \le \eta \le 1\}$. It is obvious that

$$0 \le Q(\xi/\eta) \le c,\ (\xi,\eta) \in \Omega \tag{14}$$

$$Q(\xi/\eta) = c,\ \eta \le \xi \le 1\,. \tag{15}$$

It can be shown that

$$\partial Q(\xi/\eta)/\partial\eta = -(\xi/\eta^2)\, G(\xi/\eta)\,, \tag{16}$$

$$\partial Q(\xi/\eta)/\partial\xi = G(\xi/\eta)/\eta\,, \tag{17}$$

from which it follows that $Q(\xi/\eta)$ is the decreasing function of η and increasing function of ξ for $\xi \le \eta \le 1$.

In solving inverse problem (12) it is convenient to eliminate the constant factor from the kernel $Q(\xi/\eta)$ given by Eq. (13) after transforming to the modified kernel

$$Q_1(\xi/\eta) = Q(1/\eta) - Q(\xi/\eta)\,, \tag{18}$$

where $Q(\xi/\eta) = c$. As a result, the right side of Eq. (12) is replaced by the function

$$\tilde{h}_1(\xi) = \tilde{h}(1) - \tilde{h}(\xi)\,, \tag{19}$$

which, in contrast to $\tilde{h}(\xi)$, vanishes everywhere except for the finite interval $0 \le \xi \le 1$. Below it is assumed that such substitution in Eq. (12) has been made and subscript 1 is omitted.

3. INVERSION ALGORITHM AND RESULTS OF NUMERICAL SIMULATION

The algorithm analogous to that developed for solving Eq. (1) and described at length in Ref. 6 can be used for inverting Eq. (12). It should be noted that this algorithm is based on approximation of the unknown function $\tilde{f}(\eta)$ by a piecewise–linear spline with subsequent transition to the Euler equation

$$(A^{\mathrm{T}}E^{-2}A + \alpha D)\, f_\alpha = A^{\mathrm{T}}E^{-2}h \tag{20}$$

for a finite–difference analog of the regularizing functional.[8] In Eq. (20) A is the algebraic matrix for Eq. (12), D is the smoothing matrix, f_α and h are the vectors of solution of Eq. (20) and initial data, $E = \mathrm{diag}\,\{e_1, \ldots, e_m\}$, e_i are the weighting coefficients proportional to the error of the ith measurement, and α is the regularization parameter. The function

$$f^{(+)}_{\alpha} = P_1 P_2 f_{\alpha} \quad (21)$$

is taken as an approximate solution to inverse problem (12). Here P_2 is the operator of projection onto a set of nonnegative functions, and the operator P_1 is found from the expression

$$P_1 f_{\alpha} = f_{\alpha} \left[\int\limits_0^1 f_{\alpha}(\eta)\, d\eta \right]^{-1} . \quad (22)$$

Transformation (21) allows us to consider the nonnegative character of the unknown solution and its normalization. In so doing the regularization parameter can be chosen on principle of minimum discrepancies[9] according to which the quantity $\alpha = \alpha_{m.d}$ is found from the condition of minimization of the functional

$$M(\alpha) = (1/2)\, \{\|Af_{\alpha} - h\| + \|Af^{(+)}_{a} - h\|\} . \quad (23)$$

Figure 1 shows the results of numerical experiment illustrating the efficiency of supplementary transformation (21) of the solution f_{α} obtained by inversion of Eq. (20). In the numerical simulation the log–normal distribution was taken as a rigorous solution f_0, and a random error, whose rms value was uniformly distributed in the interval [– ε, ε], was introduced into the initial data. Depicted in Fig. 1 is the rms error $\varepsilon_f = \|f_{\alpha} - f_0\|/\|f_0\|$ in the solution f_{α} obtained by inversion of regularized equation (20) (curve *1*). Also shown is the analogous quantity $\varepsilon^{(+)}_f$ for the solution $f^{(+)}_{\alpha}$ in the form of Eq. (21) (curve *2*) as a function of the rms error in the initial data ε. Both of these dependences were obtained for optimal values of the regularization parameter $\alpha = \alpha^*$. From Fig. 1 it is apparent that the transformation of the function f_{α} using the operators P_1 and P_2 in accordance with Eq. (21) decreases the error in the solution to the inverse problem by a factor of 1.5–2.

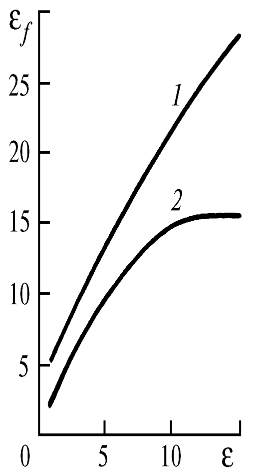

FIG. 1. Plots of the rms errors ε_f (1) and $\varepsilon^{(+)}_f$ (2) in microstructure of the medium vs the rms error in the initial data ε (%).

Figure 2 displays the behavior of the functional $M(\alpha)$ (curve *1*) and the rms error in the solution to the inverse problem $\varepsilon^{(+)}_f$ (curve *2*) as functions of α for the error in the initial data ε = 10%. As seen from Fig. 2, $\alpha_{m.d} > \alpha^*$, and the choice of the regularization parameter on principle of minimum discrepancies results in the increase of the reconstruction error $f^{(+)}_{a}$ by a factor of no more than 3%.

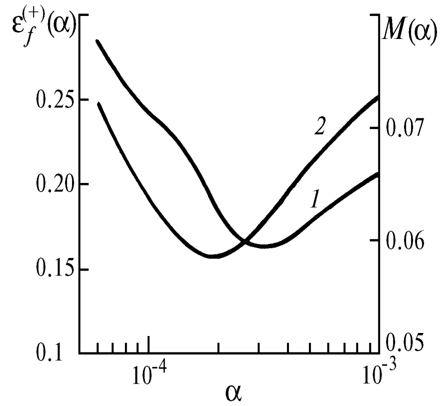

FIG. 2. The functional M(α) (curve 1, right ordinate) and the error in the solution to the inverse problem $\varepsilon^{(+)}_f(\alpha)$ (curve 2, left ordinate) as functions of the regularization parameter α for ε = 10%.

As an instance characterizing the potentialities of this method, Fig. 3 shows the result of reconstructing the two–modal distribution $f(\eta)$ which was modeled by superposition of two log–normal distributions (curve *1*). Curve *2* in Fig. 3 is the result of inverting Eq. (12) for 10% error in the input data and the optimal parameter of regularization α*. Figure 3 shows that a fraction of particles with larger modal radius is reconstructed with higher accuracy. It is accounted for by the fact that the kernel of the equation $Q_1(\varepsilon/\eta)$ vanishes for $\eta < \xi$ and increases monotonically as a function of ξ when $\xi > \eta$. Hence the larger the particle size, the larger is their contribution in the function $\tilde{h}_1(\xi)$. It should be noted that the function $\tilde{h}_1(\xi)$ contains no information about the particles with size smaller than ξ.

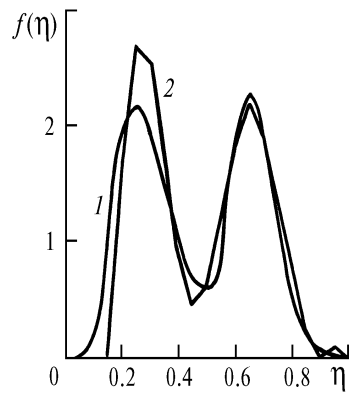

FIG. 3. Instance of reconstruction of the two–modal distribution f(η) in the numerical experiment: 1) model and 2) solution to the inverse problem for ε = 10%.

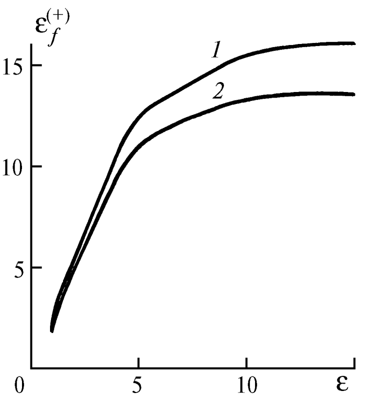

FIG. 4. The rms errors $\varepsilon_f^{(+)}$ in inversion of Eqs. (12) (curve 1) and (1) (curve 2) as functions of the rms error in the initial data ε(%).

Finally, Fig. 4 depicts a plot of the relative rms error $\varepsilon_f^{(+)}$ in the solution to inverse problem (12) (curve *1*) as a function of the rms error in the initial data ξ compared to the analogous dependence obtained for inverse problem (1) (curve *2*). Both curves have been drawn for optimal values of α*. A comparison between the dependences of Fig. 4 reveals that the inversion of Eqs. (1) and (12) yields accuracies close to each other. To put it differently, the disperse composition of the scattering media can be determined with equal efficiency based on measurements of both angular intensity distribution and spatial irradiance distribution with proper choice of radiation sources. The choice of a preferential method is directly related to its possible experimental realization. It should also be taken into account that in contrast to the method proposed in Ref. 3, the method under study is, as follows from Eq. (4), sensitive to spatial inhomogeneities of the extinction coefficient. However, this disadvantage turns out to be a positive factor which provides the possibility of reconstructing the extinction coefficient profile from measurements of the OTF of a medium.

REFERENCES

1. V.V. Veretennikov, Opt. Atmos. Okeana **6**, No 4, 250–254 (1993).
2. V.F. Belov, A.G. Borovoi, N.I. Vagin, and S.N. Volkov, Izv. Akad. Nauk SSSR, Fiz. Atmos. Okeana **20**, No. 3, 323–327 (1984).
3. N.I. Vagin and V.V. Veretennikov, Izv. Akad. Nauk SSSR, Fiz. Atmos. Okeana **25**, No. 7, 723–731 (1989).
4. L.S. Dolin, Izv. Vyssh. Uchebn. Zaved. Radiofiz. **9**, No. 1, 61–67 (1966).
5. D.M. Bravo–Zhivotovskii, L.S. Dolin, A.G. Luchinin, and V.A. Savel'ev, Izv. Akad. Nauk SSSR, Fiz. Atmos. Okeana **5**, No. 2, 160–167 (1969).
6. A.G. Borovoi, N.I. Vagin, and V.V. Veretennikov, Opt. Spektrosk. **61**, No. 6, 1326–1330 (1986).
7. E.P. Zege and A.A. Kokhanovskii, Opt. Spektrosk. **72**, No. 1, 220–226 (1992).
8. A.N. Tikhonov and V.Ya. Arsenin, *Methods of Solution of Ill–Posed Problems* (Nauka, Moscow, 1979), 285 pp.
9. V.P. Tanana, *Methods of Solution of Operator Equations* (Nauka, Moscow, 1981), 156 pp.